ELECTRONIC SUPPORTING INFORMATION

Arene C-H activation by gold(III): Solvent-enabled proton shuttling, and observation of a pre-metallation Au-arene intermediate

Luca Rocchigiani,[a] Julio Fernandez–Cestau,[a] Peter H. M. Budzelaar[b,*] and Manfred Bochmann[a,*]

[a]School of Chemistry, University of East Anglia, Norwich Research Park, Norwich NR4 7TJ, UK.
[b]Department of Chemical Sciences, Federico II University of Naples, Via Cintia, 80126 Napoli, Italy. E-mail: p.budzelaar@unina.it.

1. General Considerations

When required, manipulations were performed by using standard Schlenk techniques under dry N_2 or in a MBraun Unilab glovebox with a high capacity recirculator (<1.0 ppm O_2 and H_2O). All solvents were dried by means of the appropriate drying agent and distilled. Methylene chloride–d_2 and chlorobenzene–d_5 (Apollo Scientific) were stored in the glovebox over activated 4 Å molecular sieves. (C^N^C)AuCl (**1a**),[1] (C^N^C)AuOH,[2] (C^N^C)AuC_6F_5 (**1b**),[2] (C^N^C)Au(*p*–C_6H_4F) (**1c**),[2] and $[H(OEt_2)_2][H_2N\{B(C_6F_5)_3\}_2]$[3] were synthesized according to literature procedures. (C^N^C)Au(C_6H_5) (**1d**) has been synthesized by adapting previously reported procedures in 87% yield.[2]

Protodeauration experiments were performed within the glovebox under an anaerobic and anhydrous atmosphere, by dissolving the desired gold complex (5 to 10 mg) and 1.0 molar equiv of $[H(OEt_2)_2][H_2N\{B(C_6F_5)_3\}_2]$ in approximately 0.6 mL of dry CD_2Cl_2 or chlorobenzene–d_5 within a J-Young NMR tube.

^{1}H, ^{1}H PGSE, ^{19}F, ^{13}C{^{1}H}, *J*–resolved ^{13}C, ^{1}H COSY, ^{1}H NOESY, ^{1}H EXSY, ^{1}H,^{13}C HMQC, coupled ^{1}H,^{13}C HMQC and ^{1}H,^{13}C HMBC NMR experiments have been recorded on a Bruker DPX–300 spectrometer equipped with a ^{1}H,BB smartprobe and Z-gradients. ^{1}H NMR spectra are referenced to the residual protons of the deuterated solvent. ^{13}C NMR spectra are referenced to the D-coupled ^{13}C signals of the solvent. ^{19}F NMR spectra are referenced to an external standard of $CFCl_3$.

2. NMR data

(C^N^C)Au(C_6H_5) **1d**. ^{1}H NMR (300.13 MHz, CD_2Cl_2, 297K, *J* values in Hz): 7.76 (t, $^3J_{HH}$ = 7.9, 1H, H1), 7.69 (dd, $^3J_{HH}$ = 8.0, $^4J_{HH}$= 1.2, 2H, H11), 7.52 (d, $^3J_{HH}$ = 8.2, 2H, H5), 7.48 (d, $^4J_{HH}$ = 2.0, 2H, H8), 7.41 (d, $^3J_{HH}$ = 7.9, 2H, H2), 7.34 (m, 2H, H12), 7.24 (m, 3H, H6+H13), 1.26 ppm (s, 18H, –CMe_3). ^{13}C{^{1}H} NMR (75.47 MHz, CD_2Cl_2, 297K): 168.3 (s, C9), 163.1 (s, C3), 154.3 (s, C7), 147.8 (s, C10), 147.2 (s, C4), 141.6 (s, C1), 134.4 (s, C11), 132.3 (s, C8), 128.5 (s, C12), 124.7 (s, C5), 124.6 (s, C13), 123.3 (s, C6), 116.0 (s, C2), 35.1 (s, *C*Me_3), 30.9 ppm (s, C*Me*$_3$). Anal. Calcd. (Found) for $C_{31}H_{32}AuN$: C 60.49 (60.13), H 5.24 (5.13), N 2.28 (2.71).

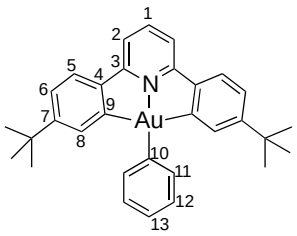

[(C^N^CH)AuCl(OEt$_2$)][$H_2N\{B(C_6F_5)_3\}_2$] **2a**

1) K.-H. Wong, K.-K. Cheung, M. C.-W. Chan, C.–M. Che, *Organometallics* 1998, **17**, 3505.
2) D. A. Rosca, D. A. Smith, M. Bochmann, *Chem. Commun*. 2012, **48**, 7247.
3) S. J. Lancaster, A. Rodriguez, A. Lara-Sanchez, M. D. Hannant, D. A. Walker, D. L. Hughes, M. Bochmann, *Organometallics* 2002, **21**, 453.

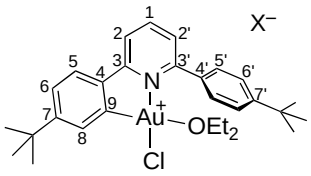

^{1}H NMR (300.13 MHz, CD_2Cl_2, 297K, J values in Hz): δ 8.27 (t, $^{3}J_{HH}$ = 7.9, 1H, H1), 7.98 (d, $^{3}J_{HH}$ = 7.9, 1H, H2), 7.76 (AB system, 4H, H5'+H6'), 7.71 (d, $^{4}J_{HH}$ = 1.3, 1H, H8), 7.66 (d, $^{3}J_{HH}$ = 7.9, 1H, H2'), 7.55 (dd, $^{3}J_{HH}$ = 8.1, $^{4}J_{HH}$ = 1.3, 1H, H6), 7.50 ($^{3}J_{HH}$ = 8.1, 1H, H5), 5.67 (br, NH_2), 1.40 (s, 9H, CMe_3′), 1.37 ppm (s, 9H, CMe_3). ^{19}F NMR (282.4 MHz, CD_2Cl_2, 297K, J values in Hz): δ –132.9 (d, $^{3}J_{FF}$ = 19.3, 2F, *o*–F $H_2N\{B(C_6F_5)_3\}_2$), –160.2 (7, $^{3}J_{FF}$ = 20.8, 1F, *p*–F $H_2N\{B(C_6F_5)_3\}_2$), –165.6 (m, 2F, *m*–F $H_2N\{B(C_6F_5)_3\}_2$). Selected $^{13}C\{^{1}H\}$ NMR (75.47 MHz, C_6D_5Cl, 297K): δ 162.1 (s, C3), 158.6 (s, C7), 157.3 (s, C3'), 157.0 (s, C7′), 143.5 (s, C1), 136.1 (s, C4), 134.4 (s, C4'), 130.9 (s, C6'), 129.7 (s, C8), 127.9 (buried under solvent, C6), 125.0 (buried under solvent, C2'+C5'), 119.5 (s, C2), 36.3 (s, *C*Me_3), 35.3 (s, *C*Me_3′), 30.6 ppm (s, C*Me*$_3$+ C*Me*$_3$′).

[(C^N^CHAu$(C_6F_5)(Et_2O)$][$H_2N\{B(C_6F_5)_3\}_2$] **2b**

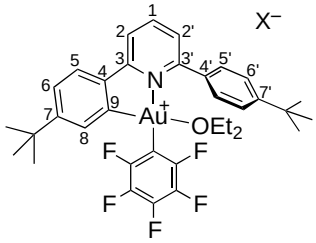

^{1}H NMR (300.13 MHz, CD_2Cl_2, 297K, J values in Hz): δ 8.30 (t, $^{3}J_{HH}$ = 7.9, 1H, H1), 8.06 (d, $^{3}J_{HH}$ = 7.9, 1H, H2), 7.88 (d, $^{3}J_{HH}$ = 8.5, 2H, H5'), 7.81 (br d, 3H H6'+H2'), 7.69 (d, $^{3}J_{HH}$ = 8.3, 1H, H5), 7.52 (brd, $^{3}J_{HH}$ = 8.3, 1H, H6), 6.54 (brs, 1H, H8), 5.68 (brs, NH_2), 1.37 (s, 9H, CMe_3′), 1.17 (s, 9H, CMe_3). ^{19}F NMR (282.36 MHz, CD_2Cl_2, 297K, *J* values in Hz): δ –121.6 (br, *o*–F Au–C_6F_5), –133.0 (br d, $^{3}J_{FF}$ = 19.0, *o*–F $H_2N[B(C_6F_5)_3]_2^-$), –151.3 (br, *p*–F Au–C_6F_5), –158.1 (br, *m*–F Au–C_6F_5), –160.2 (t, $^{3}J_{FF}$ = 20.4, *p*–F $H_2N[B(C_6F_5)_3]_2^-$), –165.7 ppm (m, *m*–F $H_2N[B(C_6F_5)_3]_2^-$). $^{13}C\{^{1}H\}$ NMR (75.47 MHz, CD_2Cl_2, 297K): δ 160.6 (s, C3), 159.4 (br s, C3′), 158.0 (s, C7), 156.2 (s, C7′), 147.8 (br d, $^{1}J_{CF}$ = 240.0, *o*–C $H_2N[B(C_6F_5)_3]_2^-$), 143.9 (s, C1), 139.6 (br s, C9), 139.1 (br d, $^{1}J_{CF}$ = 248.0, *p*–C $H_2N[B(C_6F_5)_3]_2^-$), 137.7 (s, C4), 136.7 (br d, $^{1}J_{CF}$ = 246.0, *m*–C $H_2N[B(C_6F_5)_3]_2^-$), 134.6 (s, C4′), 130.2 (s, C8), 129.2 (br s, C6′), 127.9 (s, C6), 127.6 (s, C5), 127.0 (br s, C5′), 126.4 (s, C2′), 119.4 (s, C2), 35.6 (s, *C*Me_3), 35.2 (s, *C*Me_3'), 30.7 (s, C*Me*$_3$'), 30.4 ppm (s, C*Me*$_3$).

[(C^N^CHAu(*p*–C_6H_4F)(Et_2O)][$H_2N\{B(C_6F_5)_3\}_2$] **2c**

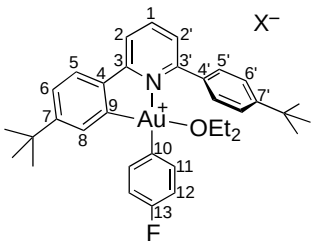

^{1}H NMR (300.13 MHz, CD_2Cl_2, 297K, J values in Hz): δ 8.21 (t, $^{3}J_{HH}$=7.9, 1H, H1), 8.07 (d, $^{3}J_{HH}$=7.9, 1H, H2), 7.78 (d, $^{3}J_{HH}$=8.6, 1H, H6'), 7.74 (d, $^{3}J_{HH}$ = 8.6, 2H, H5'), 7.71 (m, 3H, H5+H2'), 7.51 (m, 2H, H11), 7.44 (dd, $^{3}J_{HH}$ = 8.3, $^{4}J_{HH}$ = 1.5, 1H, H6), 7.11 (m, 2H, H12), 6.60 (d, $^{4}J_{HH}$ = 1.5, 1H, H8), 5.68 (br s, NH_2), 1.38 (s, 9H, CMe_3'), 1.11 ppm (s, 9H, CMe_3). ^{19}F NMR (282.36 MHz, CD_2Cl_2, 297K): –113.2 ppm (br, *p*–F), –133.0 (br d, $^{3}J_{FF}$ =

19.0, *o*–F $H_2N[B(C_6F_5)_3]_2^-$), –160.2 (t, $^3J_{FF}$ = 20.4, *p*–F $H_2N[B(C_6F_5)_3]_2^-$), –165.7 ppm (m, *m*–F $H_2N[B(C_6F_5)_3]_2^-$). $^{13}C\{^1H\}$ NMR (75.47 MHz, CD_2Cl_2, 297K, J values in Hz): 162.5 (d, $^1J_{CF}$ = 247.7, C13), 160.1 (s, C3 or C3'), 160.0 (s, C3' or C3), 156.5 (s, C7), 155.1 (s, C7'), 147.8 (br d, $^1J_{CF}$ = 240.0, *o*–C $H_2N[B(C_6F_5)_3]_2^-$), 142.5 (s, C1), 140.0 (d, $^5J_{CF}$ = 2.9, C10), 139.0 (br d, $^1J_{CF}$ = 250.0, *p*–C $H_2N[B(C_6F_5)_3]_2^-$), 138.1 (s, C4), 136.6 (br d, $^1J_{CF}$ = 250.0, *m*–C $H_2N[B(C_6F_5)_3]_2^-$), 136.1 (br s, C9), 134.8 (s, C4'), 132.5 (d, $^4J_{CF}$ = 7.0, C11), 132.0 (s, C8), 127.9 (s, C5'), 127.6 (s, C6'), 126.8 (s, C6), 126.5 (s, C2'), 126.2 (s, C5), 119.0 (s, C2), 117.2 (d, $^4J_{CF}$=21.0, C13), 35.4 (s, *C*Me_3), 35.0 (s, *C*Me_3'), 30.8 (s, –C*Me*$_3$'), 30.4 ppm (s, C*Me*$_3$).

[(C^N^CHAu(C_6H_5)(Et_2O)][$H_2N\{B(C_6F_5)_3\}_2$] **2d**

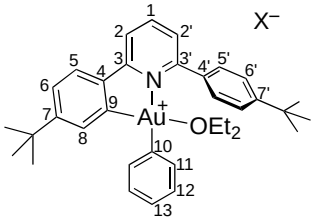

^{1}H NMR (300.13 MHz, CD_2Cl_2, 297K, *J* values in Hz): δ 8.19 (t, $^3J_{HH}$ = 8.0, 1H, H1), 8.06 (d, $^3J_{HH}$ = 8.0, 1H, H2), 7.77 (d, $^3J_{HH}$ = 8.4, 2H, H5'), 7.70 (m, 4H, H6'+H2+H5), 7.51 (br d, 2H, H11), 7.42 (dd, $^3J_{HH}$ = 8.2, $^4J_{HH}$ = 1.7, 1H, H6), 7.33 (br m, 3H, H12+H13), 6.64 (d, $^4J_{HH}$ = 1.7, 1H, H8), 5.70 (br, NH_2), 1.37 (s, 9H, CMe_3´), 1.08 ppm (s, 9H, CMe_3).

[(C^N^CHAu(C_6F_5)][$H_2N\{B(C_6F_5)_3\}_2$] **3b**

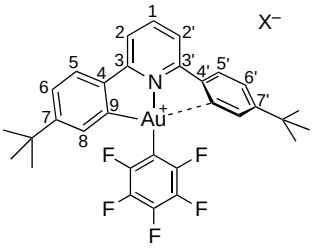

^{1}H NMR (300.13 MHz, CD_2Cl_2, 297K, J values in Hz: δ 8.42 (t, $^3J_{HH}$ = 8.0, 1H, H1), 8.18 (br d, $^3J_{HH}$ = 7.5, 2H, H5'), 8.07 (d, $^3J_{HH}$ = 8.0, 1H, H2), 8.02 (m, 3H, H2'+H6'), 7.72 (d, $^3J_{HH}$ = 7.8, 1H, H5), 7.54 (br d, $^3J_{HH}$ = 7.8, 1H, H6), 6.74 (br d, 1H, H8), 5.67 (br s, –NH_2), 1.31 (s, 9H, CMe_3'), 1.21 ppm (s, CMe_3). ^{19}F NMR (282.36 MHz, CD_2Cl_2, 297K, J values in Hz): δ –120.2 (br, *o*–F Au–C_6F_5), –133.0 (br d, $^3J_{FF}$=19.0, *o*–F $H_2N[B(C_6F_5)_3]_2^-$), –151.0 (br, *p*–F Au–C_6F_5), –158.8 (br, *m*–F Au–C_6F_5), –160.2 (t, $^3J_{FF}$=20.4, *p*–F $H_2N[B(C_6F_5)_3]_2^-$), –165.7 ppm (m, *m*–F $H_2N[B(C_6F_5)_3]_2^-$). $^{13}C\{^1H\}$ NMR (75.47 MHz, CD_2Cl_2, 297K, *J* values in Hz): δ 159.5 (s, C7 or C3), 159.4 (s, C3 or C7), 157.3 (s, C7'), 156.0 (s, C3'), 152.5 (br s, C9), 147.8 (br d, $^1J_{CF}$ = 240.0, *o*–C $H_2N[B(C_6F_5)_3]_2^-$), 144.8 (s, C1), 139.7 (s, C4'), 139.0 (br d, $^1J_{CF}$ = 250.0, *p*–C $H_2N[B(C_6F_5)_3]_2^-$), 138.2 (br s, C6'), 136.6 (br d, $^1J_{CF}$ = 250.0, *m*–C $H_2N[B(C_6F_5)_3]_2^-$), 135.6 (s, C4), 130.5 (s, C8), 128.5 (s, C5), 128.3 (s, C6), 123.7 (s, C2'), 120.4 (s, C2), 119.6 (s, C5'), 36.1 (s, *C*Me_3), 35.3 (s, *C*Me_3'), 30.4 (s C*Me*$_3$ or C*Me*$_3$'), 30.3 ppm (s C*Me*$_3$' or C*Me*$_3$).

3. Relevant NMR spectra

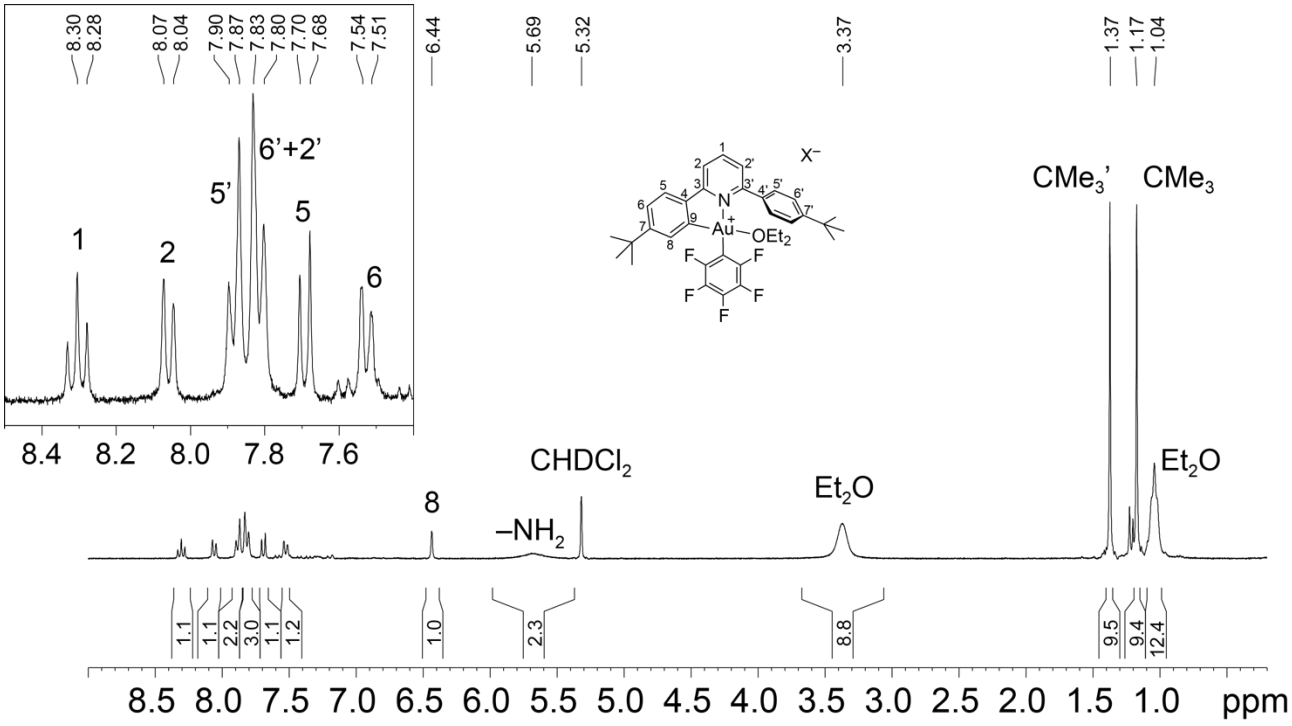

Figure S1. ^{1}H NMR spectrum of **2b** (300.13 MHz, 297K, CD_2Cl_2).

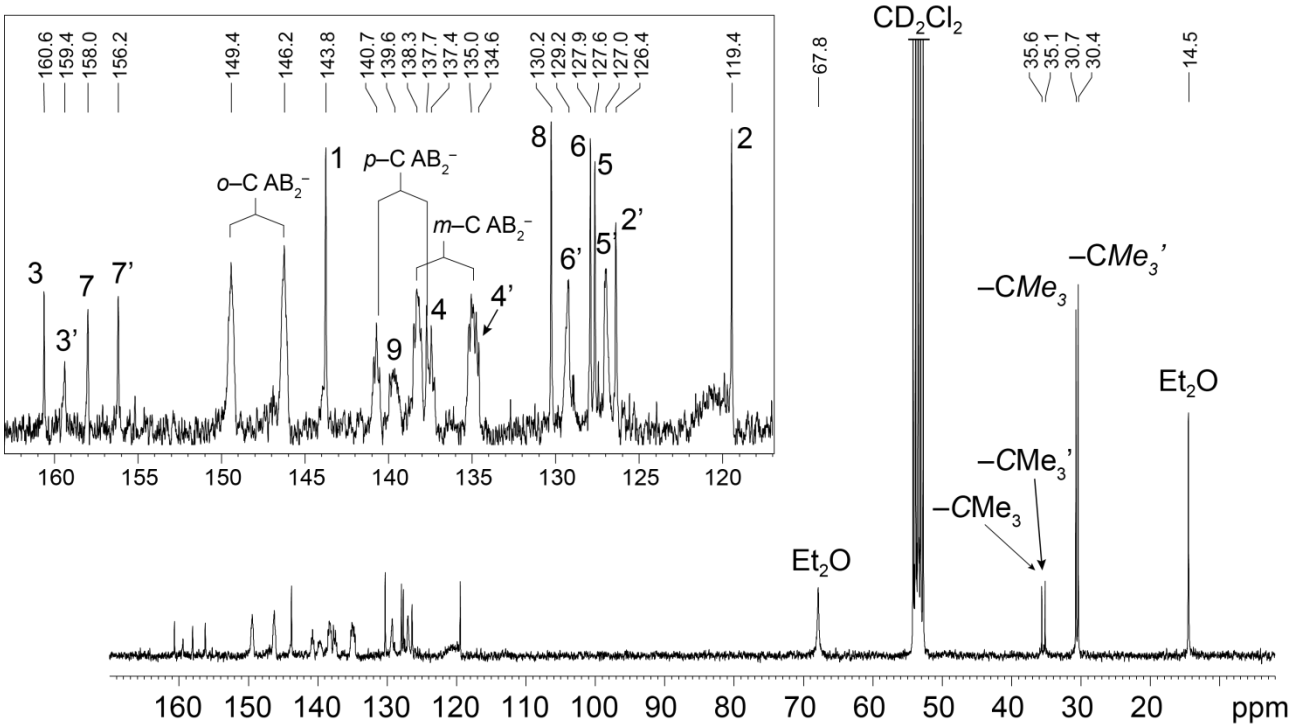

Figure S2. $^{13}C\{^{1}H\}$ NMR spectrum of **2b** (75.47 MHz, 297K, CD_2Cl_2); $AB_2^- = H_2N\{B(C_6F_5)_3\}_2^-$.

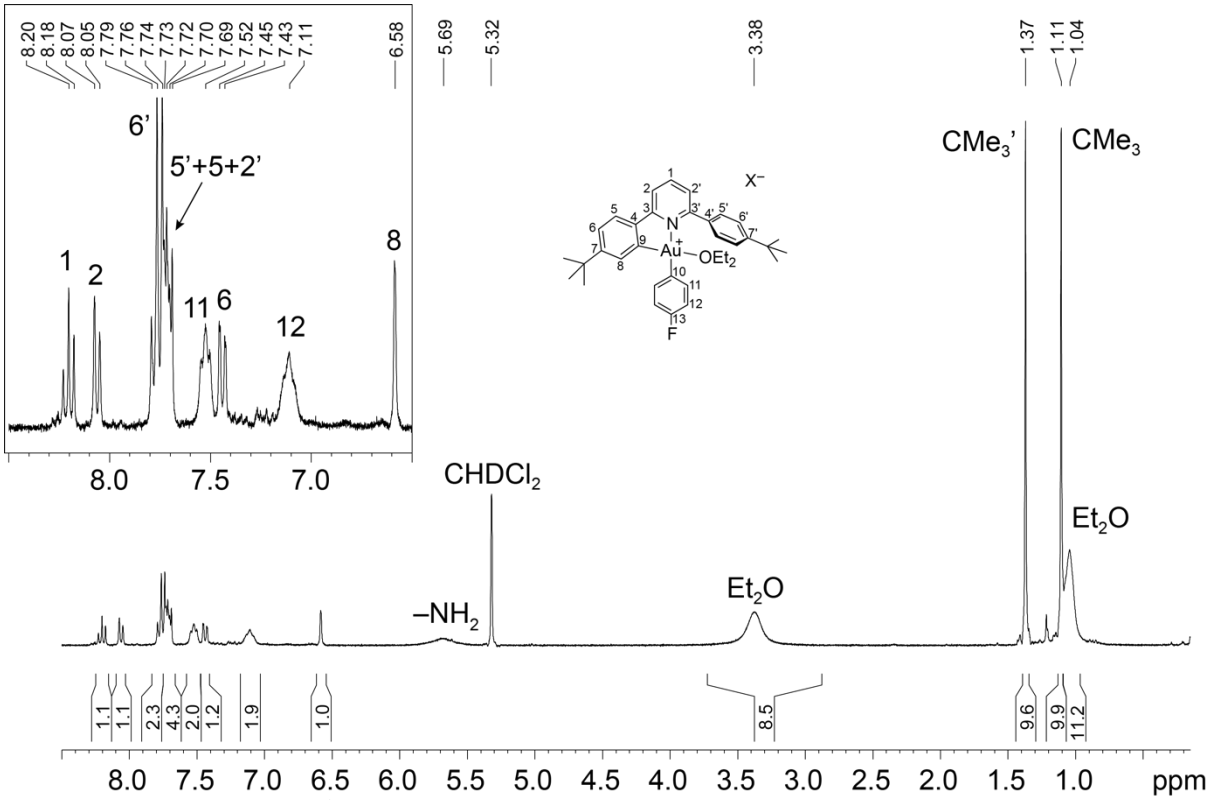

Figure S3. ^{1}H NMR spectrum of **2c** (300.13 MHz, 297K, CD_2Cl_2).

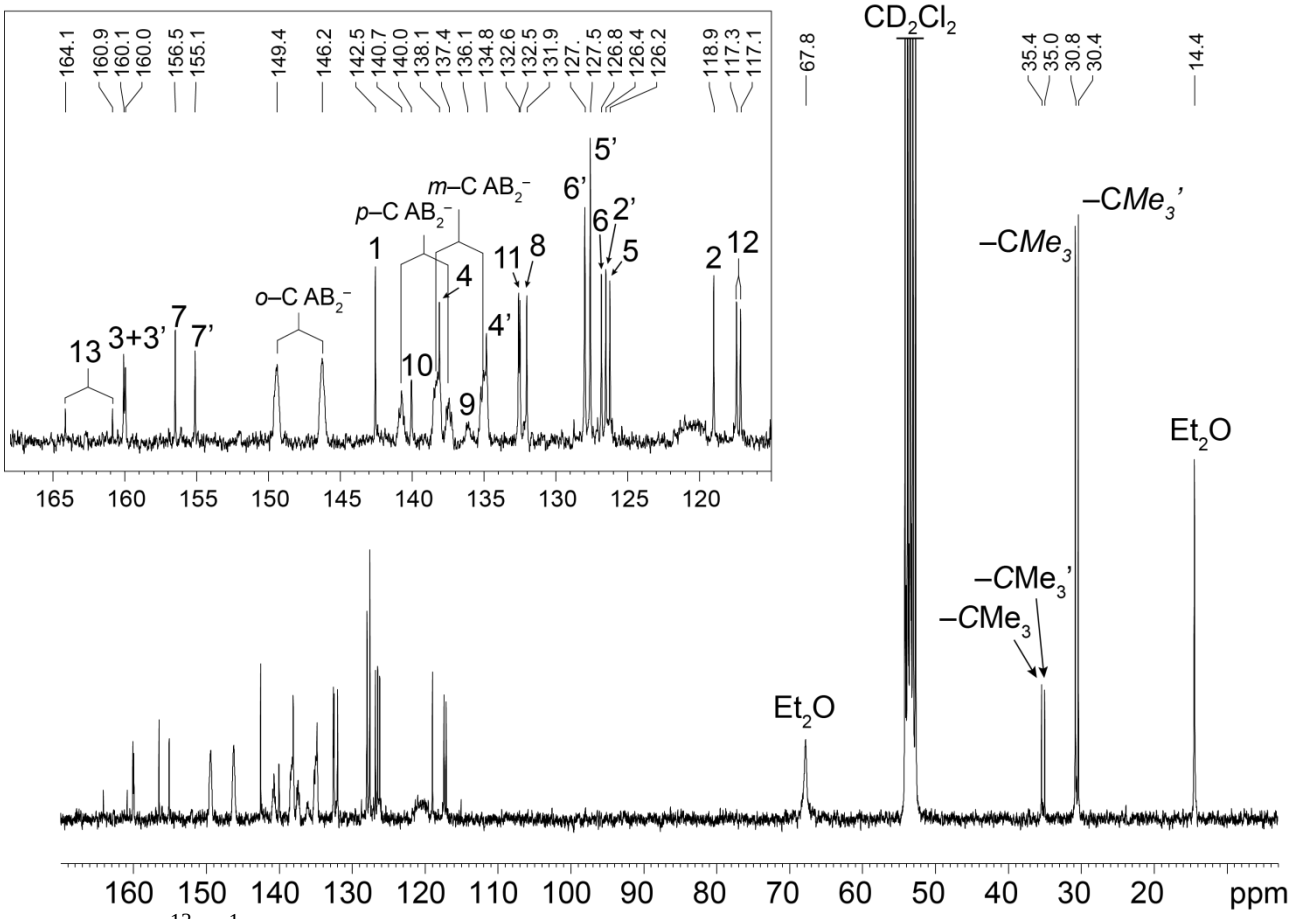

Figure S4. $^{13}C\{^{1}H\}$ NMR spectrum of **2c** (75.47 MHz, 297K, CD_2Cl_2); $AB_2^- = H_2N\{B(C_6F_5)_3\}_2^-$.

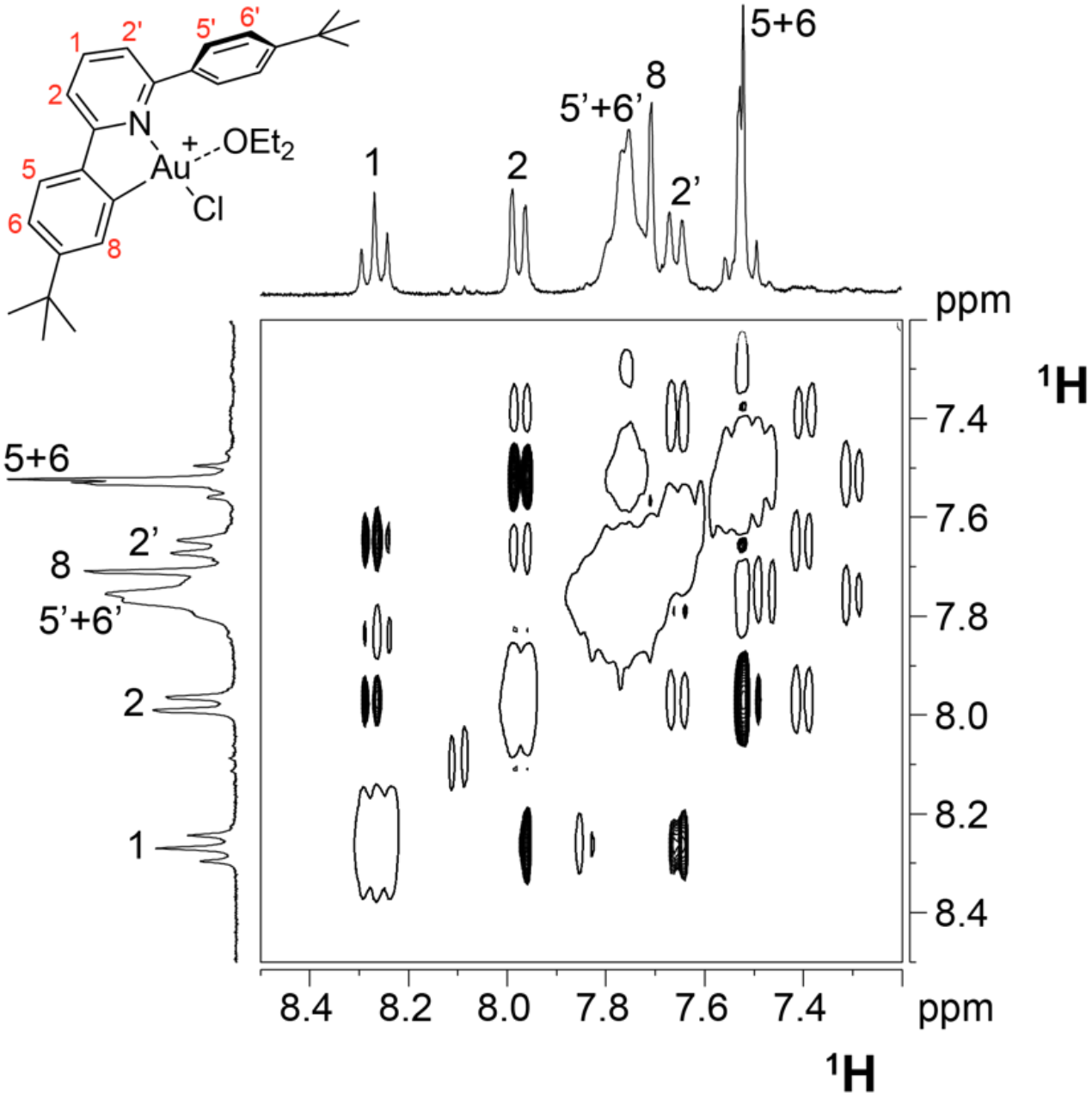

Figure S5. A section of the ^{1}H NOESY spectrum of complex **2a** showing the presence of chemical exchange between cyclometallated and protodeaurated aryl moieties (τ_M=0.8 s, CD_2Cl_2, 297K).

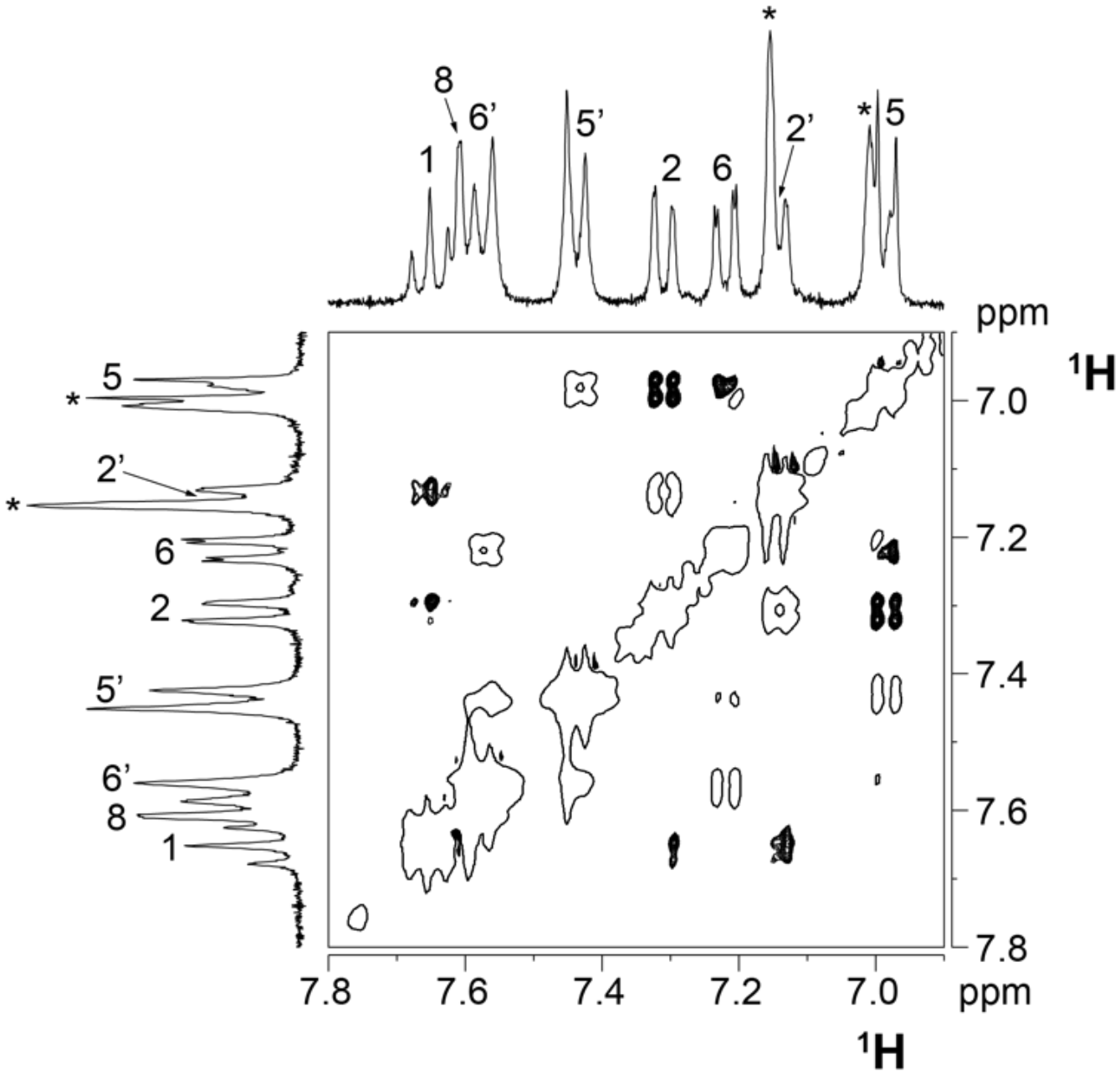

Figure S6. A section of the ^{1}H NOESY spectrum of complex **2a** (τ_M=0.8 s, C_6D_5Cl, 297K); asterisks denote residual of protonated solvent.

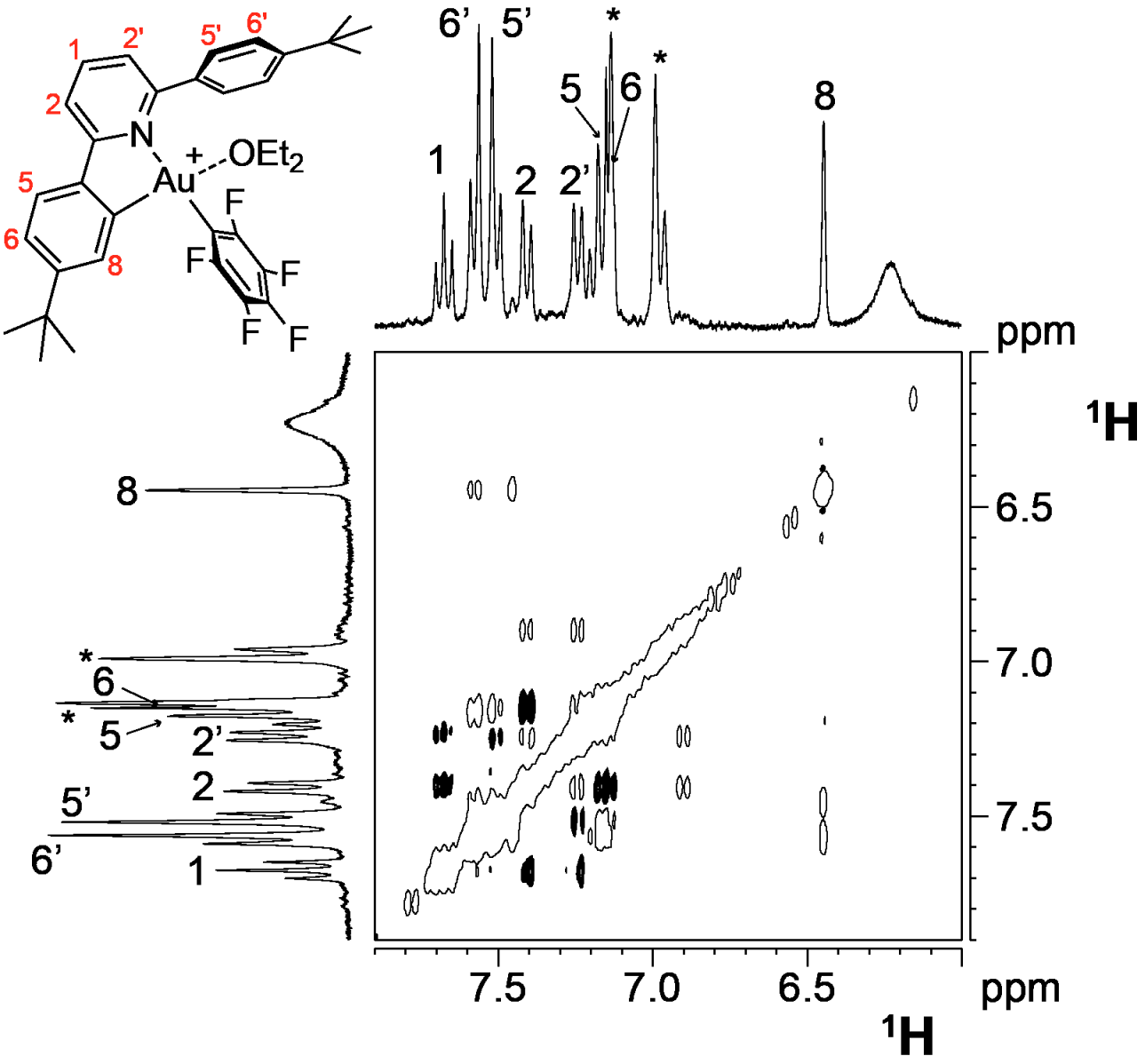

Figure S7. A section of the ^{1}H NOESY spectrum of complex **2b** (τ_M=0.8 s, C_6D_5Cl, 297K); asterisks denote residual of protonated solvent.

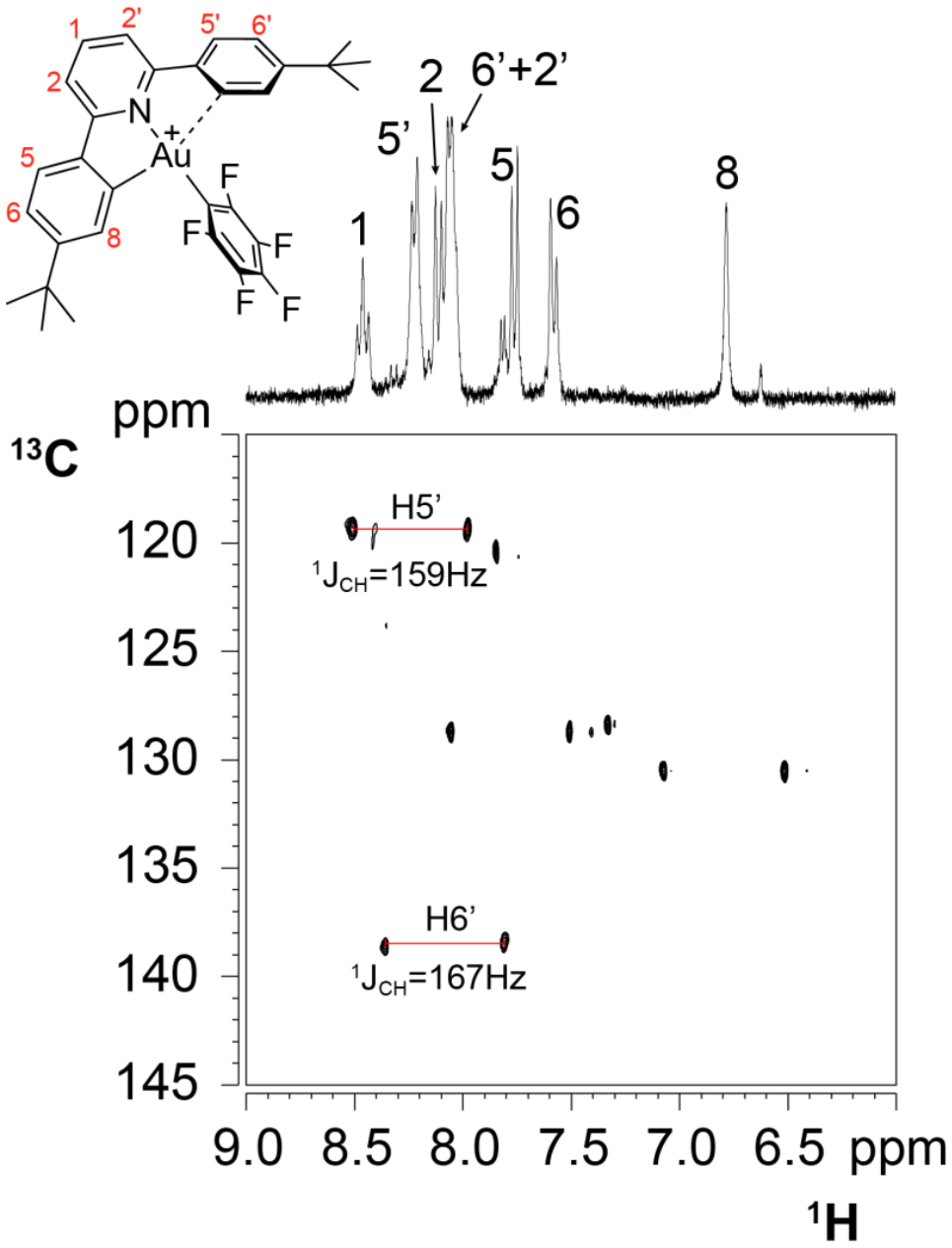

Figure S8. A section of the coupled $^{1}H,^{13}C$ HMQC NMR spectrum of complex **2b** obtained after removal of Et_2O (CD_2Cl_2, 297K).

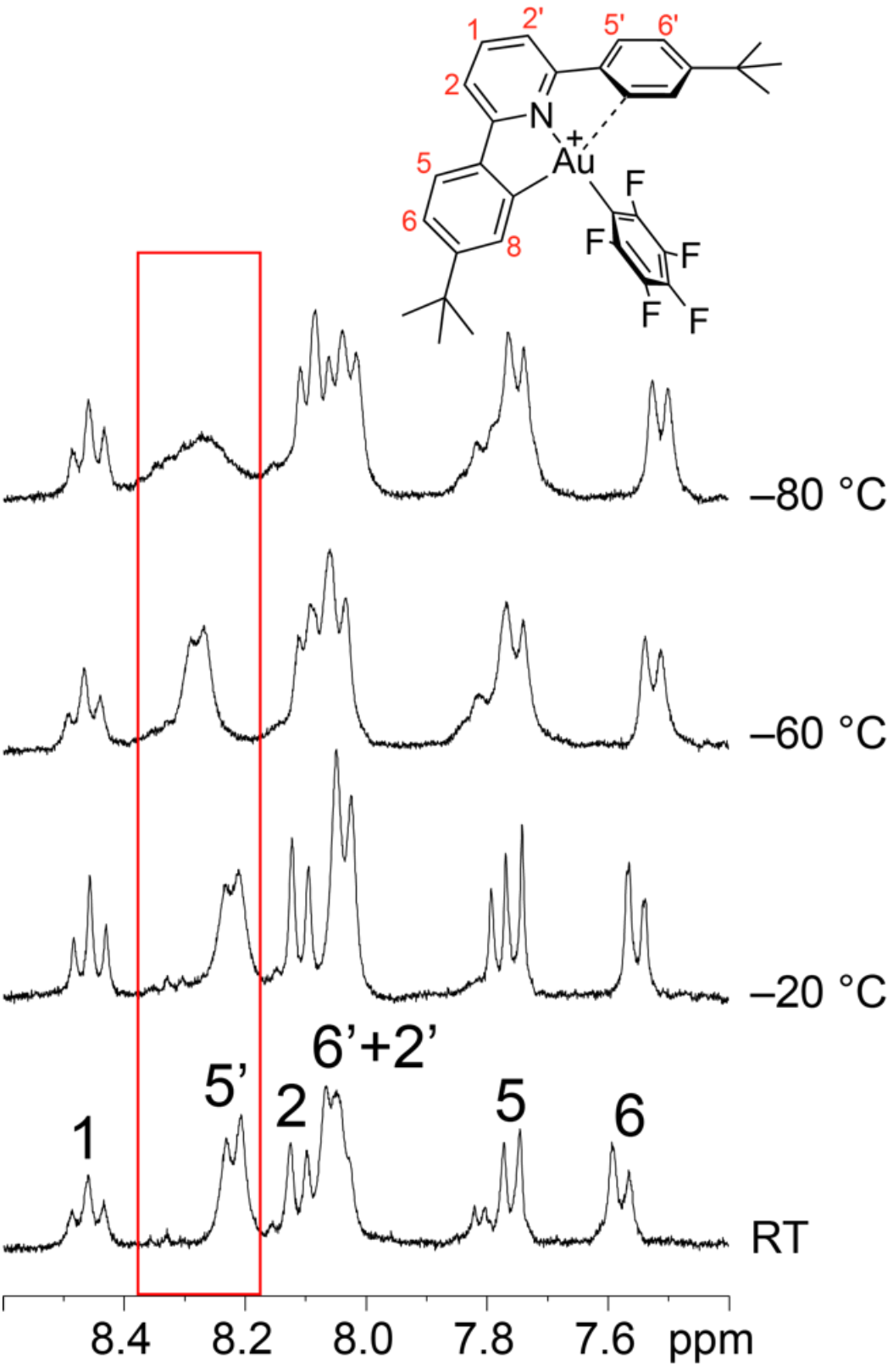

Figure S9. Temperature dependence of the aromatic region of the ^{1}H NMR spectrum of Et_2O–free **2b** complex (CD_2Cl_2).

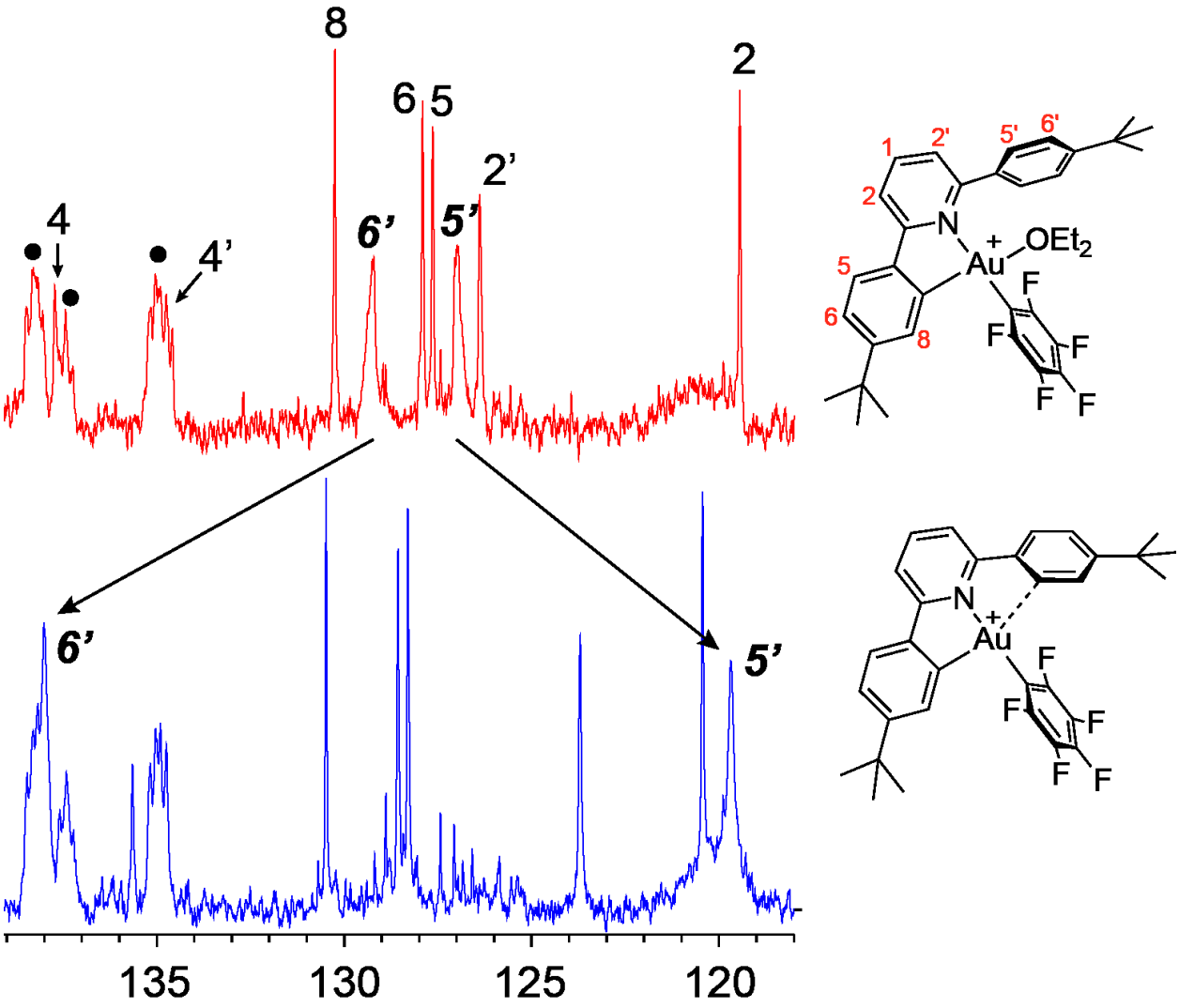

Figure S10. Evolution of a section of the $^{13}C\{^{1}H\}$ NMR spectrum of **2b** upon removal of Et_2O (297 K, methylene chloride–d_2); black dots indicate C–F signals due to the counterion.

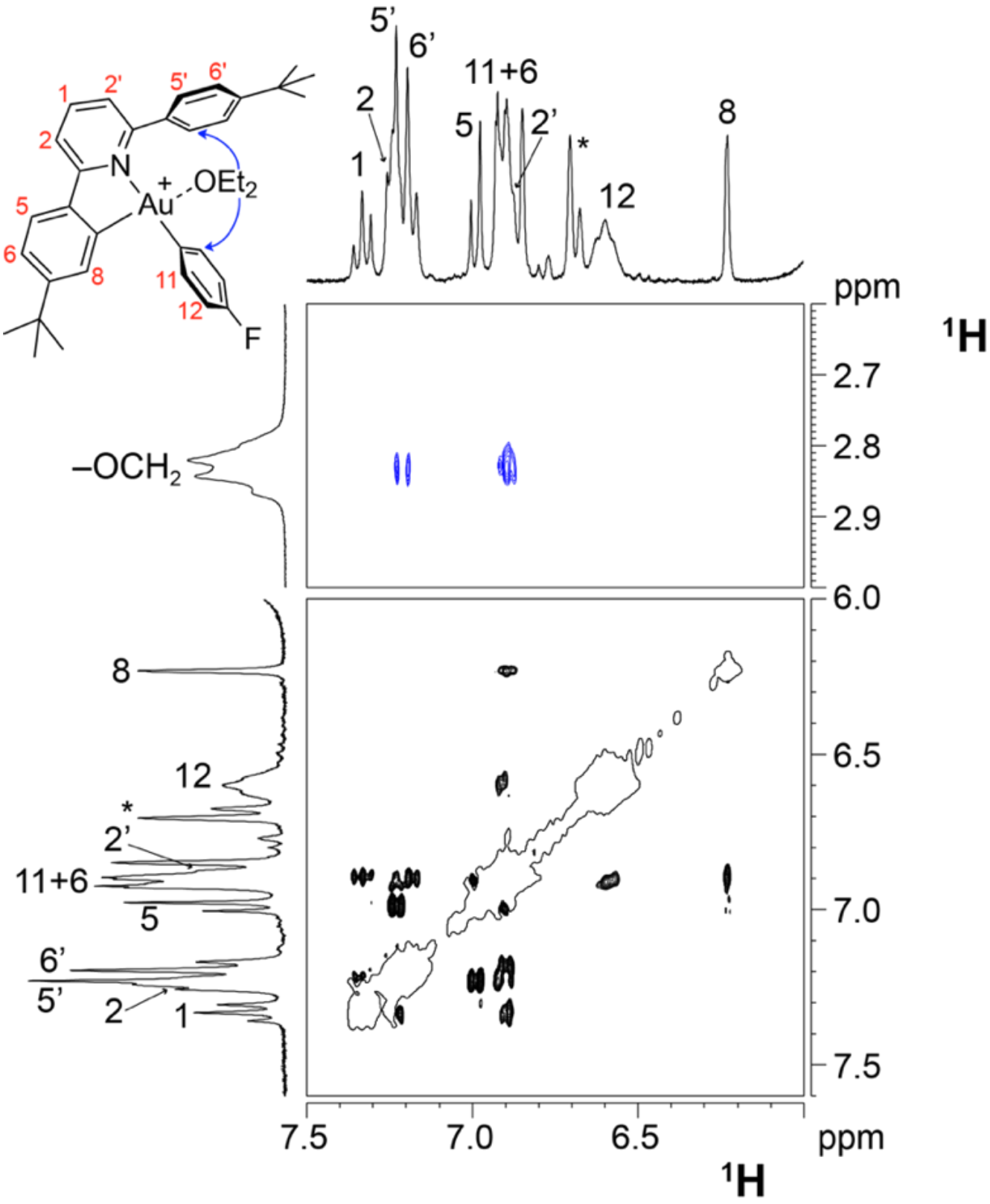

Figure S11. Two sections of the ^{1}H NOESY spectrum of complex **2c** (τ_M=0.8 s, C_6D_5Cl, 297K); asterisks denote residual of protonated solvent.

4. Diffusion NMR experiments

^{1}H PGSE measurements were performed by using a double stimulated echo sequence with longitudinal eddy current delay on a Bruker DRX 300 spectrometer equipped with a smartprobe and Z-gradient coil, at 297K without spinning. The obtained intensity (*I*) *versus* gradient (*G*) data were interpolated as reported elsewhere[4] to estimate hydrodynamic volume values (V_H) of **2a** and **2b**.

2a:
V_H^0 $H_2N[B(C_6F_5)_3]_2^-$ = 740 Å^3 (derived from the X–Ray structure of {Na}{$H_2N[B(C_6F_5)_3]_2$}^{3}
V_H^0 **2a**$^+$ = 580 Å^3 (derived from the DFT–optimized structure)
Approximate V_H^0 of the ion pair = 1320 Å^3

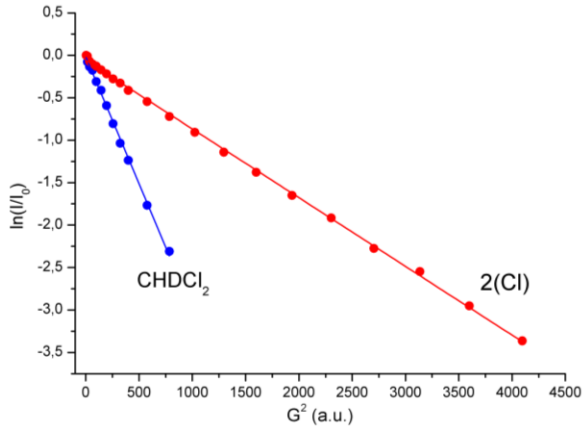

C **2a**=16.2 mM

Slope $CHDCl_2$= –2.99x10^{-3}
Slope **2a**= –8.10x10^{-2}
cr_H **2a**=34.0 Å
r_H=6.19 Å
V_H=993 Å^3

Figure S12. ln(I/I$_0$) *vs.* G^2 plot obtained for **2a** in CD_2Cl_2 at 297 K.

2b:
V_H^0 $H_2N[B(C_6F_5)_3]_2^-$ = 740 Å^3 (derived from the X–Ray structure of {Na}{$H_2N[B(C_6F_5)_3]_2$}
V_H^0 **2b**$^+$ = 670 Å^3 (derived from the DFT–optimized structure)
Approximate V_H^0 of the ion pair = 1410 Å^3

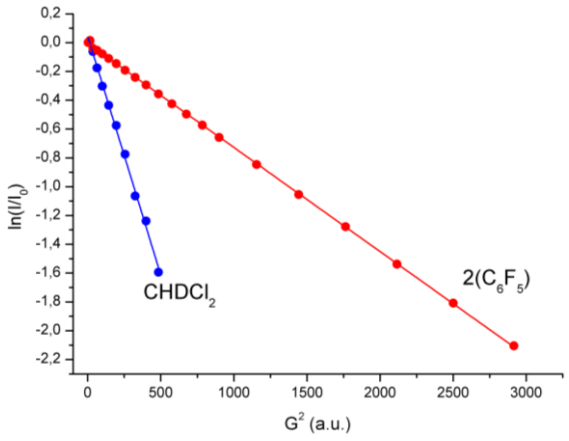

C **2b**=27.0 mM

Slope $CHDCl_2$= –3.32x10^{-3}
Slope **2b**= –7.23x10^{-2}
cr_H **2b**=42.0 Å
r_H=7.43 Å
V_H=1720 Å^3

Figure S13. ln(I/I$_0$) *vs.* G^2 plot obtained for **2b** in CD_2Cl_2 at 297 K.

4) (a) Macchioni, A.; Ciancaleoni, G.; Zuccaccia, C.; Zuccaccia, C. *Chem. Soc. Rev.* **2008**, *37*, 479. (b) Zuccaccia, D.; Macchioni, A. *Organometallics* **2005**, *24*, 3476.

5. EXSY NMR Measurements

Two-dimensional ^{1}H EXSY measurements were performed by using the *pfg* version of the standard ^{1}H NOESY sequence (noesygptp). Different values of spectral width, relaxation delay, number of transients and mixing time were used according to the sample concentration and temperature. Microscopic first-order rate constant (k_1, s^{-1}) at different mixing time values (τ_M, s) were obtained by integration of diagonal (I_{AA}, I_{BB}) and cross (I_{AB}, I_{BA}) peaks relative to the exchanging signals and applying the following relationship:

$$k_1 = \frac{1}{\tau_M} ln \frac{r+1}{r-1}$$

where $r=(I_{AA}+I_{BB})/(I_{AB}+I_{BA})$.[5] At least two experiments with different τ_M were acquired and the rate constants were obtained as the average of all the values. Linearity of ln(r+1)/(r–1) versus τ_M has been verified at 298 and 312 K, where more data points were acquired.

Table S1. Microscopic rate constants obtained for the chemical exchange in complex **2a** at different temperatures (T) and mixing time values (τ_M).

τ_M (s)	k_1(s^{-1})	$\overline{k_1}$(s^{-1})
	T = 298.65 K	
1.4	0.48	
1.2	0.49	
1.0	0.48	
0.8	0.57	0.51±0.05
	T = 312.45 K	
0.9	0.99	
0.8	1.06	
0.7	1.09	
0.55	1.16	
0.4	1.28	1.11±0.10
	T = 323.45 K	
0.5	2.35	
0.4	2.24	
0.3	2.28	2.29±0.06
	T = 333.75 K	
0.4	4.16	
0.3	4.24	4.20±0.05
	T = 344.15 K	
0.2	6.75	
0.1	6.48	6.62±0.18

5) C. K. Perrin, T. J. Dwyer, *Chem. Rev.* 1990, **90**, 935.

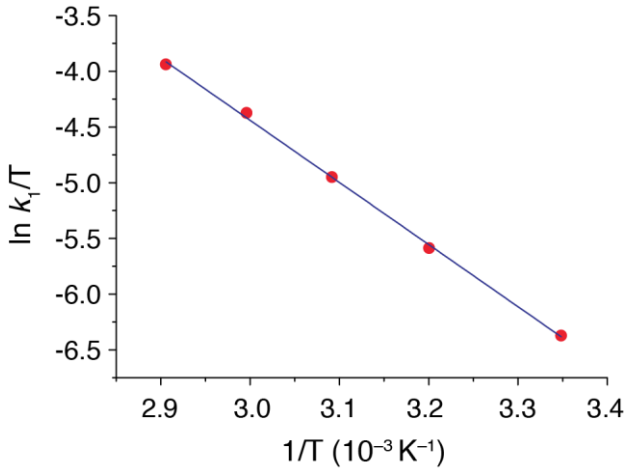

Figure S14. Eyring plot for the reversible protodeauration of **1a** in C_6D_5Cl. Linear fitting gave a $\Delta H^{\neq}$=(11.0±0.2) kcal/mol and $\Delta S^{\neq}$=(–23.0±1.0) cal mol^{-1} K^{-1}.

Table S2. Microscopic rate constants obtained for the chemical exchange in complex **2b** at different temperatures (T) and mixing time values (τ_M).

τ_M (s)	k_1(s^{-1})	$\overline{k_1}$(s^{-1})
	T = 298.65 K	
1.6	0.20	
1.3	0.14	
1.0	0.14	0.16±0.03
	T = 323.45 K	
0.6	1.27	
0.5	1.22	
0.4	1.27	1.25±0.03
	T = 344.15 K	
0.15	5.75	
0.1	6.29	6.02±0.38

6 – Details of computations

All calculations were carried out with Gaussian 09.[6] Structures were optimized at the B3LYP[7]/SVP[8] level (LANL2DZ with corresponding ECP at Au[9]) including a PCM(ChloroBenzene) solvent correction.[10] The nature of stationary points was checked by vibrational analyses. Improved single-point energies were obtained with TPSSH[11]/cc-pVTZ[12] including a PCM(ChloroBenzene) correction. These were combined with a DFT-D3 dispersion correction[13] and with the thermal corrections (enthalpy and entropy) at 323 K, obtained from the B3LYP/SVP vibrational analyses; entropy contributions were scaled by 0.67 to account for reduced freedom in the condensed phase.[14] Figure S15 (below) shows structures and relevant bond lengths for stationary points along the path for protonation of (C^N^C)AuCl (model ligand not bearing *t*Bu substituents) with $H(OMe_2)_2^+$ (model for $H(OEt_2)_2^+$). Chemical shifts were calculated using the GIAO method[15] at the TPSSH/cc-pVTZ level, using Me_4Si as reference for ^1H and ^{13}C, and $CFCl_3$ for ^{19}F; calculated chemical shifts for $(C^N^CH)Au(C_6F_5)^+$ species are collected in Figure S16. Table S3 contains total energies and thermal corrections for all species studied; an xyz archive containing all relevant coordinates is provided separately.

[6] Frisch, M. J.; Trucks, G. W.; Schlegel, H. B.; Scuseria, G. E.; Cheeseman, J. R.; Scalmani, G.; Barone, V.; Mennucci, B.; Petersson, G. A.; Nakatsuji, H.; Caricato, M.; Li, X.; Hratchian, H. P.; Izmaylov, A. F.; Bloino, J.; Zheng, G.; Sonnenberg, J. L.; Hada, M.; Ehara, M.; Toyota, K.; Fukuda, R.; Hasegawa, J.; Ishida, M.; Nakajima, T.; Honda, Y.; Kitao, O.; Nakai, H.; Vreven, T.; Montgomery, J. A. J.; Peralta, J. E.; Ogliaro, F.; Bearpark, M.; Heyd, J. J.; Brothers, E.; Kudin, K. N.; Staroverov, V. N.; Kobayashi, R.; Normand, J.; Raghavachari, K.; Rendell, A.; Burant, J. C.; Iyengar, S. S.; Tomasi, J.; Cossi, M.; Rega, N.; Millam, J. M.; Klene, M.; Knox, J. E.; Cross, J. B.; Bakken, V.; Adamo, C.; Jaramillo, J.; Gomperts, R.; Stratmann, R. E.; Yazyev, O.; Austin, A. J.; Cammi, R.; Pomelli, C.; Ochterski, J. W.; Martin, R. L.; Morukuma, K.; Zakrzewski, V. G.; Voth, G. A.; Salvador, P.; Dannenberg, J. J.; Dapprich, S.; Daniels, A. D.; Farkas, O.; Foresman, J. B.; Ortiz, J. V.; Ciolowski, J.; Fox, D. J. *Gaussian 09*, B.01; Gaussian, Inc.: Wallingford CT, 2009.

[7] (a) Becke, A. D., *J. Chem. Phys.* **1993,** *98*, 1372-1377; (b) Becke, A. D., *J. Chem. Phys.* **1993,** *98*, 5648-5652; (c) Lee, C. T.; Yang, W. T.; Parr, R. G., *Phys. Rev. B* **1988,** *37*, 785-789.

[8] Schäfer, A.; Horn, H.; Ahlrichs, R., *J. Chem. Phys.* **1992,** *97*, 2571-2577.

[9] Hay, P. J.; Wadt, W. R., *J. Chem. Phys.* **1985,** *82*, 299-310

[10] (a) Miertus, S.; Scrocco, E.; Tomasi, J., *Chem. Phys.* **1981,** *55*, 117-129; (b) Miertus, S.; Tomasi, J., *Chem. Phys.* **1982,** *65*, 239-245; (c) Tomasi, J.; Mennucci, B.; Cammi, R., *Chem. Rev.* **2005,** *105*, 2999-3093; (d) Scalmani, G.; Frisch, M. J., *J. Chem. Phys.* **2010,** *132*

[11] Tao, J. M.; Perdew, J. P.; Staroverov, V. N.; Scuseria, G. E., *Phys. Rev. Lett.* **2003,** *91*, 146401

[12] (a) Dunning, T. H., *J. Chem. Phys.* **1989,** *90*, 1007-1023; (b) Woon, D. E.; Dunning, T. H., *J. Chem. Phys.* **1993,** *98*, 1358-1371; (c) Peterson, K. A.; Puzzarini, C., *Theor. Chem. Acc.* **2005,** *114*, 283-296

[13] Grimme, S.; Antony, J.; Ehrlich, S.; Krieg, H., *J. Chem. Phys.* **2010,** *132*, 154104

[14] (a) Tobisch, S.; Ziegler, T., *J. Am. Chem. Soc.* **2004,** *126*, 9059-9071; (b) Raucoules, R.; de Bruin, T.; Raybaud, P.; Adamo, C., *Organometallics* **2009,** *28*, 5358-5367

[15] Ditchfield, R., *Mol. Phys.* **1974,** *27*, 789-807; (b) Wolinski, K.; Hinton, J. F.; Pulay, P., *J. Am. Chem. Soc.* **1990,** *112*, 8251-8260

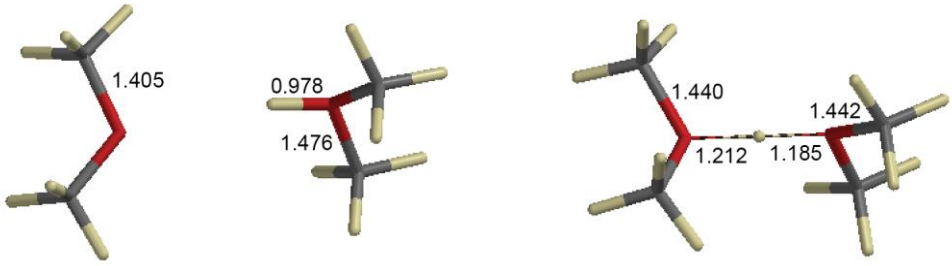

OMe2, H+_OMe2, H+_OMe2_2

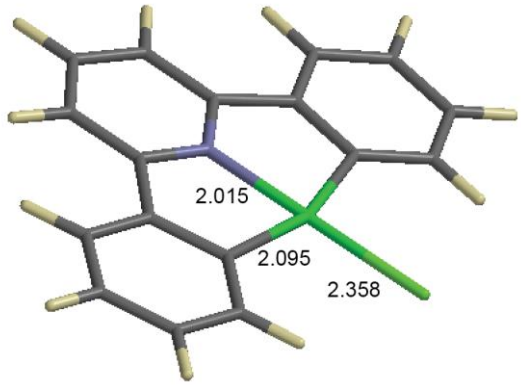

LAuCl

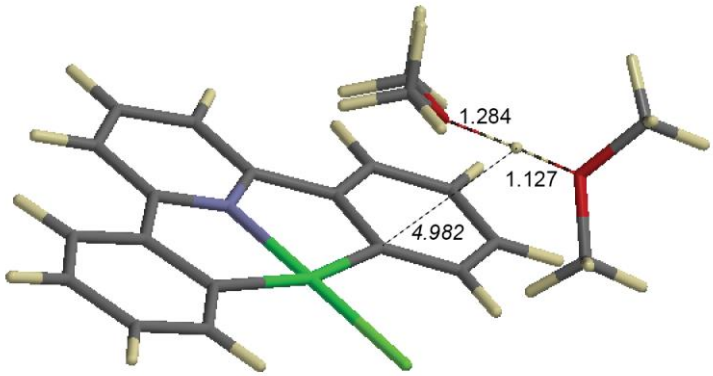

LAuCl__H+_OMe2_2

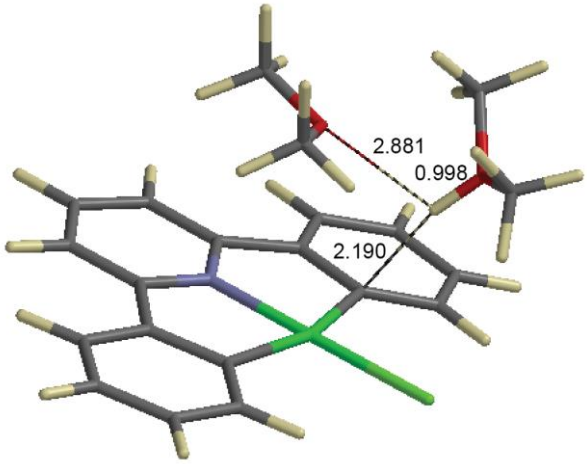

LAuCl__H+_OMe2_2_TS

Figure S15. Calculated stationary points along the path for protonation of (C^N^C)AuCl by $H(OMe_2)_2^+$. Bond lengths in Å.

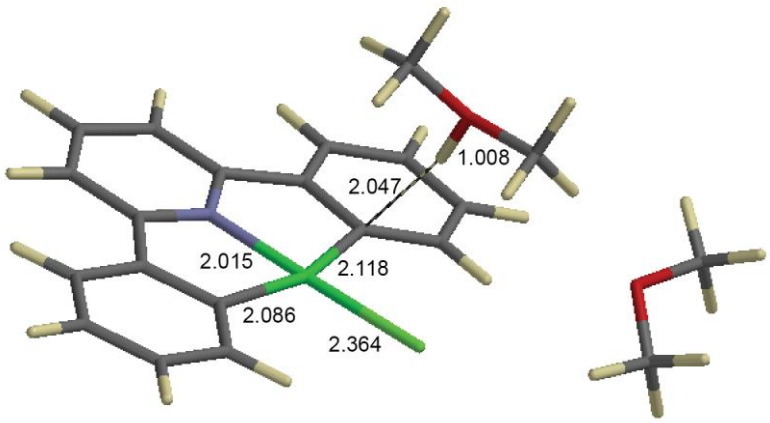

LAuCl__H+_OMe2__OMe2

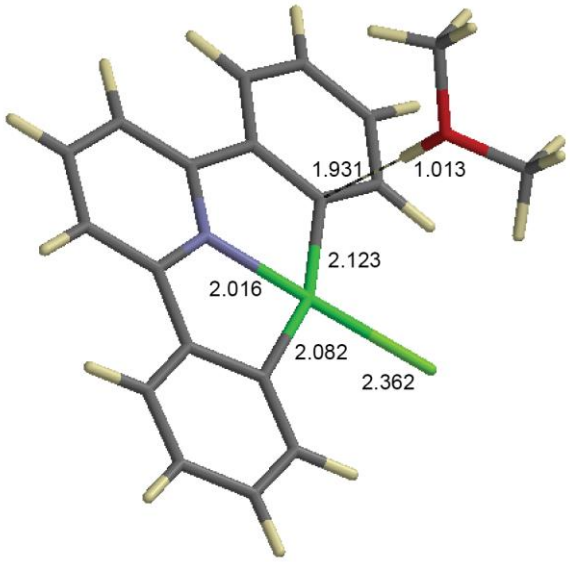

LAuCl__H+_OMe2

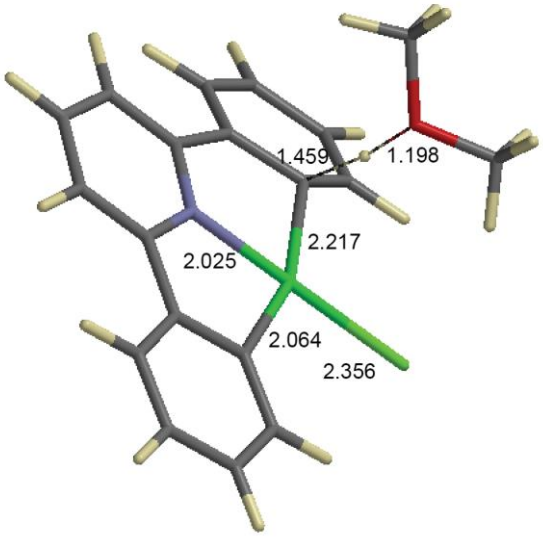

LAuCl_H+_OMe2_TS

Figure S15 (cont'd). Calculated stationary points along the path for protonation of (C^N^C)AuCl by $H(OMe_2)_2^+$. Bond lengths in Å.

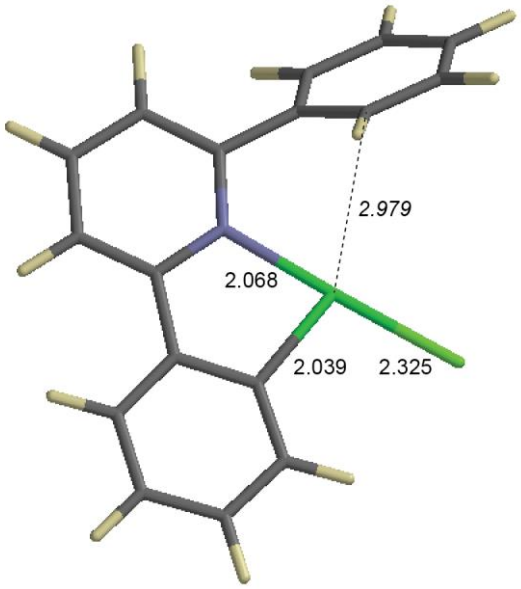

LHAu+_Cl

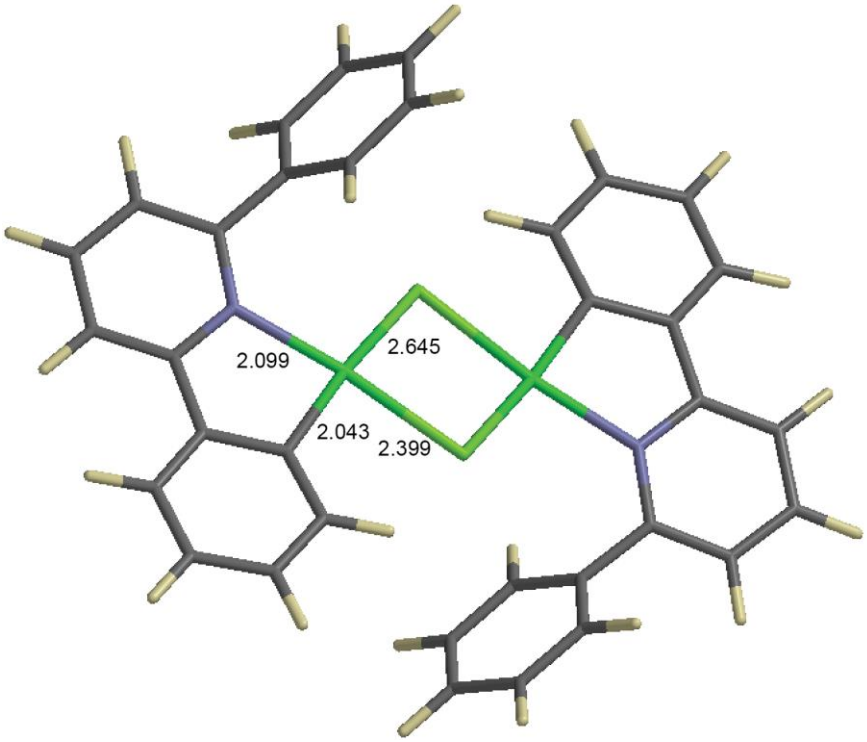

LHAuCl_2_2+

Figure S15 (cont'd). Calculated stationary points along the path for protonation of (C^N^C)AuCl by $H(OMe_2)_2^+$. Bond lengths in Å.

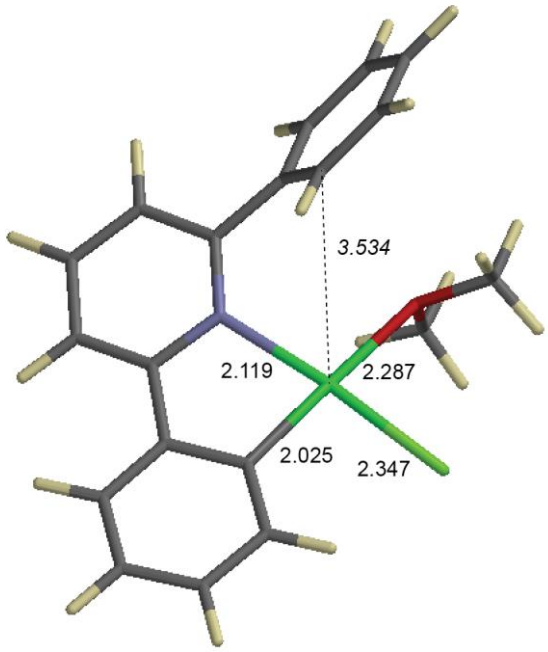

LHAu+_Cl_OMe2

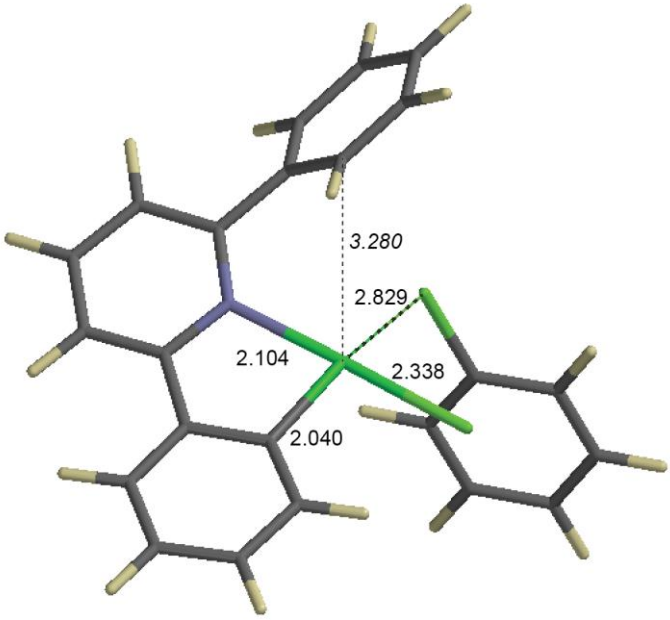

LHAu+_Cl_ClPh

Figure S15 (cont'd). Calculated stationary points along the path for protonation of (C^N^C)AuCl by $H(OMe_2)_2^+$. Bond lengths in Å.

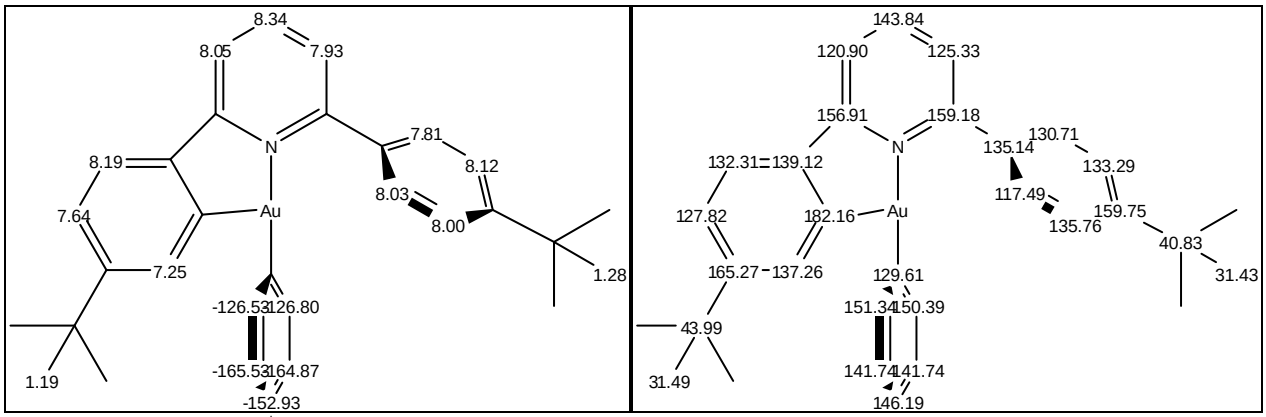

$(C\text{^}N\text{^}CH)Au(C_6F_5)^+$

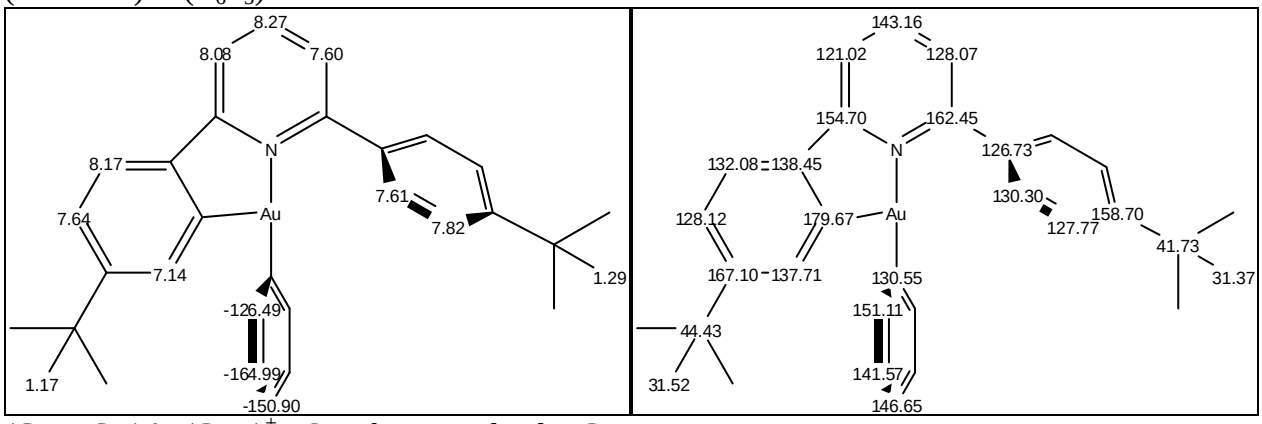

$(C\text{^}N\text{^}CH)Au(C_6F_5)^+$ TS with perpendicular C_6H_4tBu group

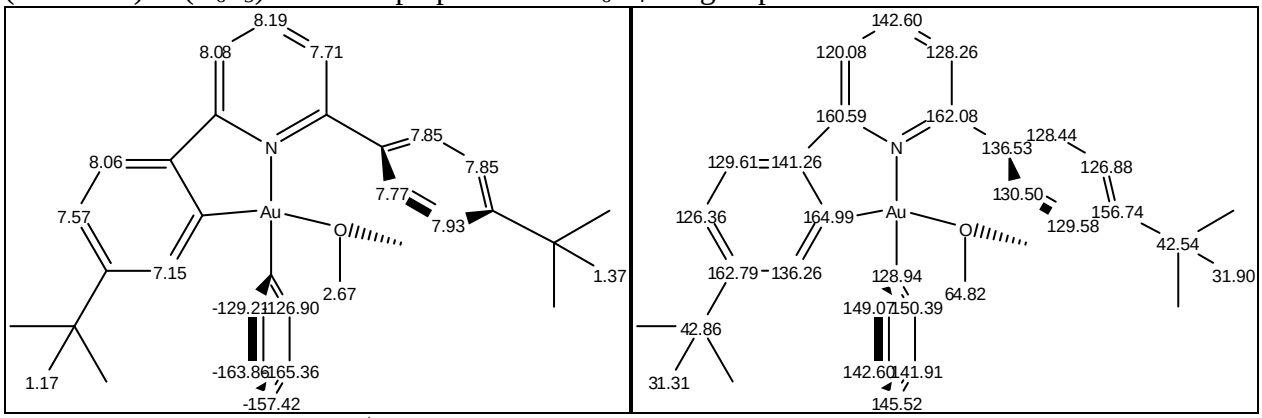

$(C\text{^}N\text{^}CH)Au(C_6F_5)(OMe_2)^+$

Figure S16. Calculated ^{13}C (left) and ^{1}H and ^{19}F (right) chemical shifts for $(C\text{^}N\text{-}CH)Au(C_6F_5)^+$ species.

Table S3. Total energies and thermal corrections.

Name	Formula	E_{elec} B3LYP	ΔH_{corr} 323 K	$T\Delta S_{corr}$ 323 K	E_{elec} TPSSH	DFTD3	G	on scale	rel kcal/mol
TMS	C4H12Si	-449.00327	0.15764	0.04780	-449.29532	-0.00692	-449.17664		
OMe2	C2H6O	-154.91169	0.08508	0.03309	-155.09304	-0.00250	-155.03263		
H+_OMe2	C2H7O	-155.30356	0.09925	0.03517	-155.48704	-0.00324	-155.41459		
H+_OMe2_2	C4H13O2	-310.25180	0.18366	0.05216	-310.61118	-0.01008	-310.47255		
OEt2	C4H10O	-233.49343	0.14445	0.04137	-233.76290	-0.00616	-233.65233		
H+_OEt2	C4H11O	-233.88991	0.15834	0.04356	-234.16266	-0.00737	-234.04088		
H+_OEt2_2	C8H21O2	-467.41383	0.30360	0.06451	-467.95002	-0.02398	-467.71361		
PhH	C6H6	-232.08645	0.10661	0.03633	-232.34665	-0.00419	-232.26858		
ClPh	C6H5Cl	-691.55304	0.09835	0.03947	-691.98175	-0.00573	-691.91558		
LAuCl {+ H+_OMe2_2}	C17H11AuClN	-1304.24069	0.25044	0.06753	-1305.45387	-0.02818	-1305.27685	-1305.27685	8.68
LAuCl__H+_OMe2_2	C21H24AuClNO2	-1614.49938	0.43734	0.10117	-1616.06852	-0.04609	-1615.74505	-1305.27250	11.41
LAuCl__H+_OMe2_2_TS	C21H24AuClNO2	-1614.47818	0.43807	0.09850	-1616.04795	-0.05626	-1615.73214	-1305.25959	19.51
LAuCl__H+_OMe2__OMe2	C21H24AuClNO2	-1614.48061	0.43889	0.10275	-1616.05036	-0.05111	-1615.73142	-1305.25887	19.97
LAuCl {+ H+_OMe2 + OMe2}	C17H11AuClN	-1304.24069	0.25044	0.06753	-1305.45387	-0.02818	-1305.27685	-1305.25152	24.58
LAuCl__H+_OMe2	C19H18AuClNO	-1459.56067	0.35114	0.08466	-1460.95323	-0.04208	-1460.70089	-1305.26097	18.65
LAuCl_H+_OMe2_TS	C19H18AuClNO	-1459.55580	0.34539	0.08223	-1460.94740	-0.04256	-1460.69966	-1305.25975	19.42
LHAu+_Cl	C17H12AuClN	-1304.66472	0.26267	0.07223	-1305.87230	-0.02935	-1305.68737	-1305.28008	6.65
LHAu+_Cl_ClPh	C23H17AuCl2N	-1996.22037	0.36321	0.09378	-1997.85275	-0.04569	-1997.59807	-1305.27520	9.72
LHAuCl_2_2+	C34H24Au2Cl2N2	-2609.33283	0.52757	0.12131	-2611.74508	-0.07652	-2611.37531	-1305.28037	6.48
LHAu+_Cl_OMe2	C19H18AuClNO	-1459.59489	0.35096	0.08454	-1460.98016	-0.04477	-1460.73060	-1305.29069	0.00
LAuCl	C17H11AuClN	-1304.24069	0.25044	0.06753	-1305.45387	-0.02818	-1305.27685	-1305.27685	5.06
LAuCl__H+_OEt2	C21H22AuClNO	-1538.14355	0.41061	0.09280	-1539.62495	-0.04843	-1539.32494	-1305.26366	13.34
LAuCl_H+_OEt2_TS	C21H22AuClNO	-1538.13543	0.40462	0.09050	-1539.61536	-0.05006	-1539.32144	-1305.26015	15.53
LHAu+_Cl	C17H12AuClN	-1304.66472	0.26267	0.07223	-1305.87230	-0.02935	-1305.68737	-1305.27841	4.08
LHAu+_Cl_ClPh	C23H17AuCl2N	-1996.22037	0.36321	0.09378	-1997.85275	-0.04569	-1997.59807	-1305.27353	7.14
LHAuCl_2_2+	C34H24Au2Cl2N2	-2609.33283	0.52757	0.12131	-2611.74508	-0.07652	-2611.37531	-1305.27869	3.90
LHAu+_Cl_OEt2	C21H22AuClNO	-1538.16861	0.41052	0.09071	-1539.64171	-0.05423	-1539.34620	-1305.28491	0.00
LbAuCl	C25H27AuClN	-1618.52246	0.48634	0.09586	-1620.09296	-0.05421	-1619.72506	-1619.72506	9.86

Name	Formula	E_{elec} B3LYP	ΔH_{corr} 323 K	$T\Delta S_{corr}$ 323 K	E_{elec} TPSSH	DFTD3	G	on scale	rel kcal/mol
LbAuCl__H+_OMe2	C27H34AuClNO	-1773.84355	0.58715	0.11131	-1775.59341	-0.06974	-1775.15058	-1619.71066	18.89
LbAuCl_H+_OMe2_TS	C27H34AuClNO	-1773.83926	0.58122	0.11077	-1775.58827	-0.06951	-1775.15078	-1619.71086	18.77
LbHAu+_Cl	C25H28AuClN	-1618.94930	0.49856	0.10079	-1620.51478	-0.05540	-1620.13916	-1619.73187	5.58
LbHAuCl_2_2+	C50H56Au2Cl2N2	-3237.89860	0.99923	0.17310	-3241.02550	-0.13455	-3240.27679	-1619.73111	6.06
LbHAu+_Cl_OMe2	C27H34AuClNO	-1773.87810	0.58683	0.11263	-1775.62072	-0.07133	-1775.18068	-1619.74077	0.00
LbAuCl	C25H27AuClN	-1618.52246	0.48634	0.09586	-1620.09296	-0.05421	-1619.72506	-1619.72506	6.74
LbAuCl__H+_OEt2	C29H38AuClNO	-1852.42641	0.64684	0.11775	-1854.26507	-0.07662	-1853.77374	-1619.71245	14.65
LbAuCl_H+_OEt2_TS	C29H38AuClNO	-1852.41888	0.64046	0.11886	-1854.25621	-0.07704	-1853.77242	-1619.71114	15.48
LbHAu+_Cl	C25H28AuClN	-1618.94930	0.49856	0.10079	-1620.51478	-0.05540	-1620.13916	-1619.73019	3.52
LbHAuCl_2_2+	C50H56Au2Cl2N2	-3237.89860	0.99923	0.17310	-3241.02550	-0.13455	-3240.27679	-1619.72943	4.00
LbHAu+_Cl_OEt2	C29H38AuClNO	-1852.45187	0.64633	0.11936	-1854.28240	-0.08104	-1853.79709	-1619.73580	0.00
LAuI	C17H11AuIN	-855.56462	0.25022	0.07019	-1140.84533	-0.03004	-1140.67217	-1140.67217	6.87
LAuI__H+_OMe2	C19H18AuINO	-1010.88210	0.35098	0.08642	-1296.34448	-0.04418	-1296.09558	-1140.65566	17.23
LAuI_H+_OMe2_TS	C19H18AuINO	-1010.87708	0.34493	0.08537	-1296.33806	-0.04472	-1296.09505	-1140.65513	17.56
LHAu+_I	C17H12AuIN	-855.98727	0.26242	0.07443	-1141.26333	-0.03084	-1141.08161	-1140.67433	5.51
LHAuI_2_2+	C34H24Au2I2N2	-1711.96753	0.52648	0.12429	-2282.53169	-0.08093	-2282.16940	-1140.67742	3.58
LHAu+_I_OMe2	C19H18AuINO	-1010.91607	0.35101	0.08518	-1296.37010	-0.04687	-1296.12303	-1140.68312	0.00
LAuPh	C23H16AuN	-1075.62034	0.34353	0.07793	-1076.92246	-0.03759	-1076.66874	-1076.66874	15.64
LAuPh__H+_OMe2	C25H23AuNO	-1230.94059	0.44384	0.09594	-1232.42358	-0.05311	-1232.09714	-1076.65722	22.87
LAuPh_H+_OMe2_TS	C25H23AuNO	-1230.93799	0.43890	0.09284	-1232.41953	-0.05345	-1232.09629	-1076.65637	23.40
LHAu+_Ph	C23H17AuN	-1076.05491	0.35614	0.08211	-1077.34953	-0.03762	-1077.08602	-1076.67873	9.37
LHAu+_Ph_OMe2	C25H23AuNO	-1230.98721	0.44465	0.09455	-1232.45980	-0.05508	-1232.13358	-1076.69367	0.00
LAuPh_H+_OMe2_phTS	C25H23AuNO	-1230.92519	0.43850	0.09195	-1232.40858	-0.05374	-1232.08543	-1076.64551	30.22
LAu+_PhH	C23H17AuN	-1076.02438	0.35639	0.08044	-1077.33173	-0.04116	-1077.07040	-1076.66312	19.17
LAuC6H4F	C23H15AuFN	-1174.78003	0.33639	0.08012	-1176.19497	-0.03813	-1175.95040	-1175.95040	15.15
LAuC6H4F__H+_OMe2	C25H22AuFNO	-1330.09949	0.43703	0.09596	-1331.69526	-0.05340	-1331.37593	-1175.93601	24.18
LAuC6H4F_H+_OMe2_TS	C25H22AuFNO	-1330.09673	0.43168	0.09527	-1331.69109	-0.05394	-1331.37719	-1175.93727	23.39
LHAu+_C6H4F	C23H16AuFN	-1175.21328	0.34898	0.08493	-1176.62065	-0.03821	-1176.36678	-1175.95949	9.45
LHAu+_C6H4F_OMe2	C25H22AuFNO	-1330.14541	0.43741	0.09753	-1331.73092	-0.05561	-1331.41446	-1175.97454	0.00
LAuC6F5	C23H11AuF5N	-1571.39489	0.30834	0.09043	-1573.25943	-0.03965	-1573.05134	-1573.05134	10.12

Name	Formula	E_{elec} B3LYP	ΔH_{corr} 323 K	$T\Delta S_{corr}$ 323 K	E_{elec} TPSSH	DFTD3	G	on scale	rel kcal/mol
LAuC6F5__H+_OMe2	C25H18AuF5NO	-1726.71277	0.40931	0.10473	-1728.75681	-0.05485	-1728.47253	-1573.03261	21.87
LAuC6F5_H+_OMe2_TS	C25H18AuF5NO	-1726.70862	0.40379	0.10354	-1728.75111	-0.05569	-1728.47237	-1573.03246	21.97
LHAu+_C6F5	C23H12AuF5N	-1571.81933	0.32075	0.09509	-1573.67738	-0.04067	-1573.46100	-1573.05372	8.62
LHAu+_C6F5_perpTS	C23H12AuF5N	-1571.81542	0.31980	0.09225	-1573.67149	-0.04022	-1573.45372	-1573.04643	13.20
LHAu+_C6F5_OMe2	C25H18AuF5NO	-1726.75238	0.40943	0.10648	-1728.78703	-0.05843	-1728.50738	-1573.06746	0.00
LHAu+_C6F5_OMe2_a	C25H18AuF5NO	-1726.75238	0.40944	0.10590	-1728.78702	-0.05846	-1728.50699	-1573.06707	0.24
LbHAu+_C6F5	C31H28AuF5N	-1886.10330	0.55675	0.12135	-1888.31919	-0.06748	-1887.91123	-1887.91123	8.01
LbHAu+_C6F5_perpTS	C31H28AuF5N	-1886.09899	0.55566	0.12101	-1888.31286	-0.06692	-1887.90520	-1887.90520	11.79
LbHAu+_C6F5_OMe2	C33H34AuF5NO	-2041.03492	0.64545	0.13267	-2043.42722	-0.08596	-2042.95662	-1887.92399	0.00
LFAuCl	C17H9AuClF2N	-1502.56171	0.23589	0.07232	-1504.00068	-0.02922	-1503.84247	-1503.84247	4.81
LFAuCl__H+_OMe2	C19H16AuClF2NO	-1657.87894	0.33685	0.08857	-1659.49732	-0.04216	-1659.26197	-1503.82206	17.62
LFAuCl_H+_OMe2_TS	C19H16AuClF2NO	-1657.87178	0.33084	0.08687	-1659.48903	-0.04351	-1659.25991	-1503.81999	18.92
LFHAu+_Cl	C17H10AuClF2N	-1502.97790	0.24819	0.07614	-1504.41094	-0.03032	-1504.24409	-1503.83680	8.37
LFHAuCl_2_2+	C34H20Au2Cl2F4N2	-3005.96066	0.49861	0.13031	-3008.82402	-0.07902	-3008.49173	-1503.83858	7.25
LFHAu+_Cl_OMe2	C19H16AuClF2NO	-1657.91027	0.33658	0.08857	-1659.52146	-0.04582	-1659.29005	-1503.85014	0.00
LOMeAuCl	C19H15AuClNO2	-1533.12429	0.32103	0.08205	-1534.59901	-0.03554	-1534.36850	-1534.36850	8.54
LOMeAuCl__H+_OMe2	C21H22AuClNO3	-1688.44544	0.42174	0.09849	-1690.09972	-0.04896	-1689.79293	-1534.35301	18.25
LOMeAuCl_H+_OMe2_TS	C21H22AuClNO3	-1688.43956	0.41577	0.09732	-1690.09279	-0.04992	-1689.79215	-1534.35223	18.74
LOMeHAu+_Cl	C19H16AuClNO2	-1533.54874	0.33327	0.08542	-1535.01842	-0.03652	-1534.77890	-1534.37161	6.58
LOMeHAuCl_2_2+	C38H32Au2Cl2N2O4	-3067.10376	0.66876	0.14688	-3070.03794	-0.09565	-3069.56324	-1534.37434	4.87
LOMeHAu+_Cl_OMe2	C21H22AuClNO3	-1688.47829	0.42161	0.09874	-1690.12508	-0.05239	-1689.82202	-1534.38210	0.00
LCOMeAuCl	C21H15AuClNO2	-1609.31261	0.33267	0.08821	-1610.86761	-0.03861	-1610.63265	-1610.63265	5.69
LCOMeAuCl__H+_OMe2	C23H22AuClNO3	-1764.62987	0.43383	0.10320	-1766.36441	-0.05237	-1766.05209	-1610.61218	18.53
LCOMeAuCl_H+_OMe2_TS	C23H22AuClNO3	-1764.62338	0.42747	0.10266	-1766.35638	-0.05298	-1766.05068	-1610.61076	19.42
LCOMeHAu+_Cl	C21H16AuClNO2	-1609.73119	0.34466	0.09152	-1611.28059	-0.03963	-1611.03688	-1610.62960	7.60
LCOMeHAuCl_2_2+	C42H32Au2Cl2N2O4	-3219.47373	0.69219	0.15533	-3222.56646	-0.10302	-3222.08136	-1610.63340	5.22
LCOMeHAu+_Cl_OMe2	C23H22AuClNO3	-1764.66300	0.43318	0.10380	-1766.38997	-0.05529	-1766.08163	-1610.64171	0.00
ZAuCl	C16H10AuClN2	-1320.25187	0.23814	0.06752	-1321.48438	-0.02742	-1321.31889	-1321.31889	7.17
ZAuCl__H+_OMe2	C18H17AuClN2O	-1475.56982	0.33906	0.08457	-1476.98184	-0.04062	-1476.74007	-1321.30015	18.93
ZAuCl_H+_OMe2_TS	C18H17AuClN2O	-1475.56407	0.33307	0.08232	-1476.97491	-0.04169	-1476.73869	-1321.29877	19.80

Name	Formula	E_{elec} B3LYP	ΔH_{corr} 323 K	$T\Delta S_{corr}$ 323 K	E_{elec} TPSSH	DFTD3	G	on scale	rel kcal/mol
ZHAu+_Cl	C16H11AuClN2	-1320.67226	0.25055	0.07161	-1321.89858	-0.02846	-1321.72447	-1321.31718	8.24
ZHAuCl_2_2+	C32H22Au2Cl2N4	-2641.34979	0.50339	0.11835	-2643.79986	-0.07465	-2643.45041	-1321.31792	7.78
ZHAu+_Cl_OMe2	C18H17AuClN2O	-1475.60511	0.33913	0.08360	-1477.00950	-0.04385	-1476.77023	-1321.33032	0.00
HZAuCl+	C16H11AuClN2	-1320.66511	0.25182	0.06829	-1321.90042	-0.02808	-1321.72245	-1321.72245	-9.18
HZAuCl__H2+_OMe2	C18H18AuClN2O	-1475.96659	0.35371	0.08192	-1477.38186	-0.04022	-1477.12325	-1321.68333	15.36
HZAuCl_H2+_OMe2_TS	C18H18AuClN2O	-1475.95472	0.34698	0.08226	-1477.36841	-0.04205	-1477.11859	-1321.67867	18.29
HZHAu2+_Cl	C16H12AuClN2	-1321.05600	0.26414	0.07126	-1322.28586	-0.02902	-1322.09848	-1321.69120	10.43
HZHAuCl_2_4+	C32H24Au2Cl2N4	-2642.09207	0.53133	0.11725	-2644.54767	-0.07537	-2644.17027	-1321.67785	18.81
HZHAu2+_Cl_OMe2	C18H18AuClN2O	-1475.99416	0.35334	0.08253	-1477.40151	-0.04426	-1477.14774	-1321.70782	0.00

[a] For each block, reference: LHAuZ+_OR2

Table S4. Predicted substituent effects (kcal/mol) on deprotonation barriers of $[(C\text{^}N\text{-}CH)AuX]^+$.[a]

Subst at C^N^C	X	Base	$\Delta G^{\dagger}$ A-TS-D	ΔG_{rxn} A-F+H$(OR_2)_2^+$
-	Cl	OMe_2	19.42	8.68
-	Cl	OEt_2	15.53	5.06
*t*Bu	Cl	OMe_2	18.77	9.86
*t*Bu	Cl	OEt_2	15.48	6.74
F	Cl	OMe_2	18.92	4.81
COMe	Cl	OMe_2	19.42	5.69
OMe	Cl	OMe_2	18.74	8.54
-	I	OMe_2	17.56	6.87
-	C_6F_5	OMe_2	21.97	10.12
-	C_6H_5	OMe_2	23.40	15.64
-	*p*-C_6H_4F	OMe_2	23.39	15.15

[a] Free energies evaluated at 50 °C.